

Dual-function stem molecular beacons to assess mRNA expression in AT-rich transcripts of *Plasmodium falciparum*

Leyla Y. Bustamante, Almudena Crooke, Joaquín Martínez, Amalia Díez, and José M. Bautista

Universidad Complutense de Madrid, Madrid, Spain

BioTechniques 36:488-494 (March 2004)

The genome of the human malaria parasite Plasmodium falciparum is extremely AT-rich such that it is particularly difficult to design standard probes to identify and quantify specific transcripts. Biased AT genome contents (70%–80%) lead to a high proportion of short repetitions and a low free energy of binding between target sequences and their specific probes during hybridization. This causes nonspecific annealing and high background noise. We constructed molecular beacon probes with dual-function stems to avoid nonspecific detection and establish identical melting patterns for use with several fluorescent probes for the analysis of mRNA expression in P. falciparum in real-time reverse transcription PCR (RT-PCR) assays. The method proved highly efficient at detecting low transcript levels in P. falciparum microcultures. Conditions were established for two types of real-time instruments, demonstrating that molecular beacons with dual-function stems are a useful tool for the functional analysis of high AT genomes. The procedure could be adapted to high-throughput gene expression protocols for the biomolecular screening of the P. falciparum and other AT-rich genomes.

INTRODUCTION

The complete sequencing of the *Plasmodium falciparum* genome has been a milestone in our current understanding of the malaria parasite (1). One of the most characteristic features of this genome is its high AT content (70%–80% AT), and it has been established through biocomputing analysis that approximately 60% of its coding regions are of unknown function (2). Thus, the next rational step in unraveling the biology of this parasite is to ascribe functions to each genome sequence and thus take full advantage of the available sequence information. One approach to this goal is to evaluate transcriptome profiles, but traditional methods of gene expression analysis, such as Northern blot hybridization, require large-scale parasite cultures, lack sensitivity, and cannot be adapted to high-throughput screening.

Many of the limitations of these methods can be overcome by real-time reverse transcription PCR (RT-PCR). However, extremely AT-rich sequences, such as those of the *P. falciparum* genome, hinder the design of specific probes for the identification and quan-

tification of mRNA expression. Among the consequences of a high AT content is that probe-cDNA hybrids have a low free energy profile and anneal nonspecifically, producing a high fluorescence background in negative controls that lack the target cDNA.

The use of molecular beacons has been reported for the real-time detection of critical nucleic acid hybridization events (3), and they have proved successful in a variety of PCR applications (3–9). The thermodynamic properties of molecular beacons promote the formation of a hairpin in the absence of target sequence. The significant advantages of molecular beacons over conventional nucleic acid probes are their fidelity and ability to detect a single mismatch in a target (4,10,11), making them ideal for highly repetitive sequences such as those found in AT-rich genomes. Optimal performance of the molecular beacon probe essentially depends on its stem design and the establishment of accurate thermal denaturation profiles (12,13).

In the present report, we describe strategies for the design of molecular beacons to detect mRNA expression in *P. falciparum*. Special attention was

paid to the selection of optimal target areas, sequence overlapping, and criteria for fluorescence detection. In addition, attempts were made to quantify mRNA expression using minimal amounts of parasite mRNA. We then applied the whole procedure to determine the asexual stage-specific expression of the *P. falciparum* glucose-6-phosphate dehydrogenase (*g6pd*) and Fe-superoxide dismutase (*Fe-sod*) genes. Molecular beacon signals were normalized against signal from a molecular beacon identifying the 18S rRNA gene used as an internal control (14,15). The data presented validate real-time RT-PCR as a scalable high-throughput technique for accurate stage-specific quantitative expression analysis. Other possible applications include biomolecular screening using minimal amounts of malaria parasite cultures.

MATERIALS AND METHODS

Parasite Cultures

P. falciparum (strain 3D7) was cultured in human erythrocytes using standard methods (16), with the exception that the culture medium contained 0.5% AlbuMAX[®] I (Invitrogen, Carlsbad, CA, USA), instead of human serum, and 5 g/mL hypoxanthine. For all the experiments, parasites were synchronized at the ring stage with D-sorbitol (17). After synchronization, experiments were performed in 96-well plates in a final volume of 200 μ L, with a 5% hematocrit and parasitemia between 0.5%–3%.

Molecular Beacon and Primer Design

We used the Primer Express[®] v2.0 package (Applied Biosystems, Foster City, CA, USA) to select optimal positions in the primer and molecular beacon loop portions (complementary to the *P. falciparum* sequences) to amplify and detect mRNA derived from the *g6pd*, *Fe-sod*, and 18S rRNA genes. We selected the following variables from the software's "Primer and Probe Design" document, which contains the full-length coding sequence: optimal primer melting temperature (T_m),

Table 1. Primers and Molecular Beacon Probe Sequences for Real-Time RT-PCR

Set No.	Forward Primers	Reverse Primers	Molecular Beacons ^a	Gene and GenBank Accession No.
1	5'-GAAC TCCAGGAAAAACAAGTCAA-3'	5'-TTTTGACAAGTCCAAATACCTCT-3'	5'-GGGCCCTCTTAAATATCTTTTGGATCATCAGGCC-3'	<i>g6pd</i> (X74988)
2	5'-GAAC TCCAGGAAAAACAAGTCAA-3'	5'-TTTTGACAAGTCCAAATACCTCT-3'	5'-CGCGCGTCTTAAATATCTTTTGGATCATCAGGCC- CGCGCG-3'	<i>g6pd</i> (X74988)
3	5'-CAACGCTGCTCAAATATGGA-3'	5'-CATGAGGCTCACACCACA-3'	5'-CGGCC TACTTTTACTGGGATTCTATGGGACCT- GGCCG-3'	Fe- <i>sod</i> (Z49819)
4	5'-CAACGCTGCTCAAATATGGA-3'	5'-CATGAGGCTCACACCACA-3'	5'-CCCCCTACTTTTACTGGGATTCTATGGGACCT- GGGGG-3'	Fe- <i>sod</i> (Z49819)
5	5'-TGACTACGTCCTGCCCTT-3'	5'-ACAATCATCATCTTTCAATGG-3'	5'-GGGGGACACCGCCGTCGCTCCGCC-3'	18S rRNA (M19172)

All probes were labeled at the 5' end with 6-carboxyfluorescein (FAM). TAMRA was used as the 3' quencher. RT-PCR, reverse transcription PCR.
^aThe arm sequences that form the stem are underlined. Letters in bold indicate the dual-function sequence.

57°C; maximum primer T_m , 58°C; minimal primer T_m , 56°C; maximal T_m difference between primer pair, 2°C; maximum product length, 150 bp; minimal product length, 80 bp; probe T_m (referring to the loop molecular beacon), 8°–10°C higher than primers. Complementary sequences of the arms (to form the molecular beacon stem by self-annealing) at the ends of the probes were designed by adding GC to achieve a T_m of 7°–10°C below the loop T_m . This T_m was predicted by a folding program (18). The total T_m of the molecular beacon was 10°–12°C higher than that of the loop. The melting properties of the probes were those recommended by Bonnet et al. (19). Part of the arm sequence was designed to include a dual function: self-complementary to the opposite arm and complementary to the target mRNA sequence. The stem probe sequence is designed to contain 2–5 dual-function GC at the 5' or 3' ends. To achieve this, we chose optimal positions containing GC at the 5' or 3' ends from the results list of the Primer Express software. The sequences of the specific oligonucleotide and molecular beacon probes used are shown in Table 1. For the non-dual function *g6pd* probe, we chose the same sequence containing GC at the 5' or 3' ends, but used no part of this sequence to form the stem (Table 1). Probes were purchased from Isogen Life Science (Maarsse, The Netherlands), and primers were purchased from Genotek (Barcelona, Spain).

Titration of Probe Fluorescence

Because at times we needed to maintain a 5' guanine in our selected probes, which is cautioned against to prevent self-quenching of the fluorophore, we considered it necessary to titrate the fluorescence produced by each probe with the target. To do this, a conventional PCR for *g6pd* and *sod* was performed using the primers used for real-time RT-PCR. Once the PCR fragment concentration had been determined, a fixed amount of each (in the range of 10 ng/μL) was mixed with serial dilutions of the respective probe to determine the probe concentration rendering identical fluorescence. To achieve an identical amount of fluorescence for comparative analysis, the

concentrations of probes yielding the lowest fluorescence (*g6pd* non-dual function stem and *sod* heteropolymer stem) were proportionally increased in the assay with respect to the corresponding probe showing the highest fluorescence (*g6pd* dual-function stem and *sod* homopolymer stem). Real-time RT-PCR for these genes using probe concentrations rendering similar fluorescence produced identical results in terms of cycle threshold (C_t ; data not shown) to the experiments conducted with equal probe concentrations. These preliminary assays served to demonstrate that differences in fluorescence due to the yield obtained during probe synthesis or to the presence of 5' guanine do not interfere with results for different probe sequences.

Real-Time RT-PCR

Total RNA was isolated from 12 μL of infected red blood cell cultures at 4 different time points using the MagNA Pure[®] LC Instrument (Roche Applied Science, Mannheim, Germany) or the ABI PRISM[®] 6100 Nucleic Acid Preparation (Applied Biosystems).

Isolated RNA was retrotranscribed to cDNA using the High-Capacity[™] cDNA Archive Kit (Applied Biosystems) as described by the manufacturer, except that the following specific reverse primers of an annealing temperature approximately 40°C were used: *g6pd*, 5'-TTTTGACAAGTCCAA-3'; Fe-*sod*, 5'-CATGAGGCTCACCA-3'; and 18S rRNA, 5'-CCAAA-CAATTCATCATA-3'. For real-time transcript quantification, the cDNA was amplified either in the LightCycler[®] Instrument (Roche Applied Science) using the reagents of the LightCycler FastStart Master Hybridization Probes (Roche Applied Science) or in the ABI PRISM 7000 Sequence Detector (Applied Biosystems) using the reagents of the TaqMan[®] system (Applied Biosystems).

To optimize the experimental conditions for each PCR primer set, the primer concentration generating the lowest C_t and the highest reduced normalized fluorescence (ΔR_n) values was chosen. We used every possible combination of primer concentrations in the range 50–900 nM (50, 100, 300,

Table 2. Probe Sequence Assessment

Gene	Probe Definition ^a	C _t	SD
<i>g6pd</i>	Dual-Function Stem	29.49	0.167
		29.70	
		29.82	
	Non-Dual Function Stem	32.55	0.235
		32.08	
		32.31	
<i>sod</i>	Dual-Function Heteropolymer Stem	28.36	0.129
		28.38	
		28.15	
	Dual-Function Homopolymer Stem	31.20	0.134
		31.14	
		30.94	

Probes with or without a dual-function stem [using the glucose-6-phosphate dehydrogenase (*g6pd*) gene] and probes with homo- or heteropolymeric stems [using the superoxide dismutase (*sod*) gene] were compared in parallel experiments. Cycle threshold (C_t) numbers for individual reactions in triplicate experiments are given alongside their respective standard deviation (SD).

^aThe set numbers in Table 1 were used to yield these data (set number 1, dual-function stem; 2, non-dual function stem; 3, dual-function heteropolymer stem; and 4, dual-function homopolymer stem).

600, and 900 nM) with genomic DNA and cDNA in the real-time PCR assays. The optimal concentration was found to be 300 nM in each case. Similarly, 7 experimental molecular beacon concentrations (100, 150, 200, 250, 300, 350, and 400 nM) were used on DNA and cDNA at the optimal primer concentration (300 nM). We discovered that a molecular beacon concentration of 300 nM was the lowest rendering minimal C_t and ΔRn.

For the LightCycler amplifications, the LightCycler FastStart DNA Master Hybridization Probes mixture (Roche Applied Science) containing 5 mM MgCl₂ was used according to the manufacturer's instructions. Amplification and detection were performed in three stages: (i) 95°C for 10 min; (ii) 45 cycles of 95°C for 0 s (ramp 20°C/s) for denaturation, 45°C for 0 s for fluorescence detection, 55°C for 10 s for annealing (ramp 20°C/s), and 72°C for 8 s for extension (ramp 20°C); and (iii) 40°C for 1 min.

The TaqMan Universal PCR Master Mix (2×), No AmpErase[®] UNG (both from Applied Biosystems) was used for ABI PRISM 7000 amplification and detection. Real-time PCR involved 1 cycle each of 50°C for 2 min and 95°C for 10 min, followed by 45 cycles of 57°C for 1 min, 95°C for 30 s, and 45°C for 29 s for fluorescence detection.

Calculations for mRNA Expression Analysis

The ribosomal 18S rRNA signal was used to normalize against differences in RNA isolation and degradation, as well as against any possible efficiency difference in the reverse transcription reactions and PCRs. All samples were run in triplicate and quantified by normalizing the *g6pd* and *sod* signals with the 18S rRNA signal. The data were exported into Microsoft[®] Excel[®], and a standard curve was generated using

known genomic DNA concentrations and the resultant C_ts. C_t values from the *g6pd* and *Fe-sod* real-time RT-PCR signal were interpolated in their corresponding standard curve to calculate the copy number. Final results were obtained by dividing through with the expression values derived from the constitutively expressed gene (18S rRNA) according to the ABI PRISM 7700 User Bulletin 2 (Applied Biosystems).

RESULTS AND DISCUSSION

Melting Properties of the Probes

To define the experimental detection temperature during PCR cycling, we conducted a melting curve analysis of the molecular beacons. Melting curves from 40°–95°C were used to determine the temperature at which only fluorescence from the molecular beacons bound to the target is detectable. The start of the conformational transition of the probe occurred at 45°C, so we used this temperature as the experimental detection temperature, given background fluorescence levels above this temperature were high. This was subsequently confirmed by melting curve analysis in the presence of a specific PCR target product for each molecular beacon probe.

For practical purposes, all real-time RT-PCR assays were designed to follow identical cycling and temperature detection patterns such that different genes could be compared in a single experiment. Direct comparisons were made between a *g6pd* probe with a dual-function stem and an analogous construct without the dual-function stem, and between the *sod* probe with a dual-function heteropolymer stem and an analogous dual-function construct with a homopolymer stem. As seen in Table 2, the dual-function stem probe showed improved behavior over the probe lacking the dual-function stem when assessed in the same experiment, with around three earlier C_ts obtained. When we compared the heteropolymer versus the homopolymer stem probes, enhanced detection was observed during PCR, with the heteropolymer stem probe rendering 2.5 earlier C_ts. Nevertheless, standard deviations for both sets were similar, indicating that homopolymer sequences do not alter specificity but that delay in the C_ts due to sliding could occur at the stem. It should be noted, however, that it is not always possible to preserve a heteropolymer design and the dual function. In fact, the *g6pd* probe performed better using a homopolymer stem rather than a heteropolymer stem of the probe without the dual function (Table 2).

To adapt several probes to a single heat profile, our molecular beacons proved to be sufficiently flexible since their stems could be used for dual functions (see Materials and Methods). The use of dual-function stems for AT-rich targets meant that long probes could be shortened (to the length required to render an adequate T_m), and these were sufficiently plastic to incorporate the GCs needed to obtain the desired detection temperature. Within the range of detection, there was a more efficient transition of the dual-function part of the stem between the hairpin structure and target hybridization than in normal molecular beacons (Figure 1A). This was demonstrated even using the short detection cycle in the LightCycler instrument, where we observed the high efficiency of these probes. We managed to produce the same thermal cycling profile in a large

number of molecular beacon probes for the expression analysis of several *P. falciparum* genes (data not shown), despite high AT contents that prevented the use of an identical thermal profile for multiple probes using other fluorescence systems.

Quantification by Real-Time PCR

RT-PCR amplification of the specific *P. falciparum* genes using primer sets yielded single bands of the predicted size (Figure 1B). Gene specificity was confirmed by sequencing these

cloned products. Sequences were 100% homologous to *P. falciparum* sequences available from GenBank®.

Standard curves were generated using serial 10-fold dilutions (300 ng to 300 pg) of *P. falciparum* genomic DNA to determine quantitative expression levels. Under the assay conditions, the relationship between the C_t and genomic DNA was linear over the concentration range used (slope: -3.7 to -3.3). This demonstrated that each specific primer/probe set was able to accurately determine the transcript concentration in the 12- μ L sample of parasite culture, which was within the range of the standard curve (Figure 1C).

We then tested the reliability of the molecular beacon designed by performing real-time RT-PCR at the optimum conditions established to determine asexual stage-specific expression of *g6pd* and *Fe-sod* in *P. falciparum*. We used RNA from 12 μ L of infected red blood cells from synchronized cultures showing 0.5%–3% parasitemia. The reactions were performed in triplicate using the two instruments mentioned above (see Materials and Methods). The standard deviation of the C_t s was always $<0.30 C_t$.

Transcripts of *g6pd* and *Fe-sod* were detected at the three main erythrocyte stages of *P. falciparum* infection (rings, young and late trophozoites, and schizonts) at parasitemia levels as low as 0.5% in RNA from 12 μ L microcultures. The relative expression of the *g6pd* and *Fe-sod*

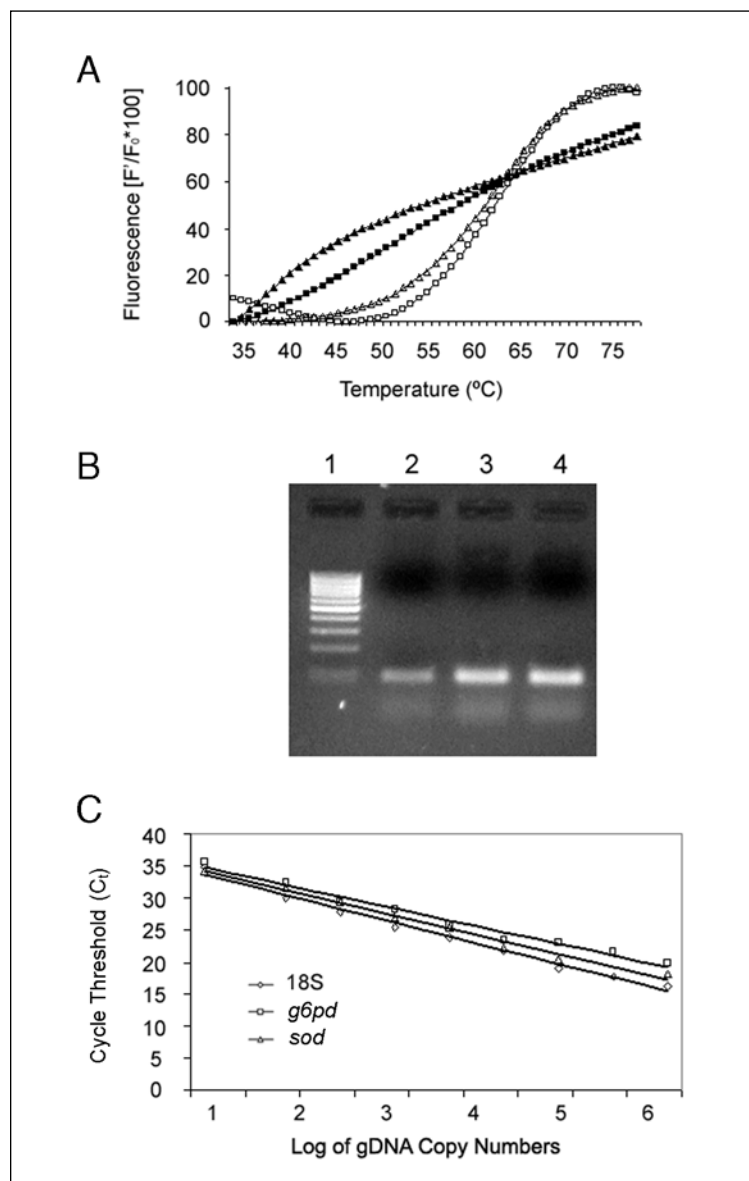


Figure 1. Behavior of molecular beacons with dual-function stems. (A) Comparative melting curves: shaded squares indicate glucose-6-phosphate dehydrogenase (*g6pd*) non-dual function stem probe without target; open squares indicate *g6pd* non-dual function stem probe in the presence of its cDNA target; shaded triangles indicate *g6pd* dual-function stem probe without target; and open triangles indicate *g6pd* dual-function stem probe in the presence of its cDNA target. (B) Reverse transcription PCR (RT-PCR) amplification yielded single bands of the expected size. Lane 1, 100-bp ladder molecular weight marker (Promega, Madison, WI, USA); lane 2, *g6pd*; lane 3, Fe-superoxide dismutase (*Fe-sod*); and lane 4, 18S rRNA. (C) Standard curves used to calculate copy numbers and determine expression levels were constructed from real-time PCR of *Plasmodium falciparum* genomic DNA (gDNA) using primer/probe sets for *g6pd* (slope: -3.30; $r^2 = 0.987$), *Fe-sod* (slope: -3.43; $r^2 = 0.991$), and 18S rRNA (slope: -3.67; $r^2 = 0.989$).

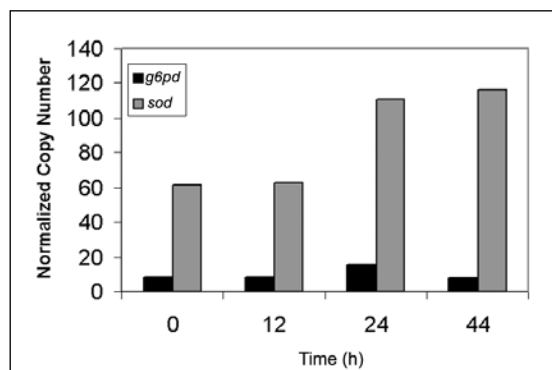


Figure 2. Asexual stage-specific expression of *g6pd* and *Fe-sod* determined in RNA isolated from *Plasmodium falciparum* microcultures. Transcripts were detected in rings (0 h), young trophozoites (12 h), late trophozoites (24 h), and schizonts (44 h). Expression levels are provided as normalized copy numbers. *g6pd*, glucose-6-phosphate dehydrogenase; *Fe-sod*, Fe-superoxide dismutase.

genes was calculated as a function of the expression of the constitutively expressed 18S rRNA gene. Distinct patterns of the level of transcription of these two genes were observed during the parasite's asexual development cycle (Figure 2). *Fe-sod* was expressed at high levels during all stages of parasite development and reached its peak of two-fold expression in late trophozoites and schizonts, compared to the minimal expression detected at the ring stage. In comparison, *g6pd* showed a low expression pattern with values corresponding to 15%–30% *Fe-sod* expression. Late trophozoites also showed peak *g6pd* expression with a quick decrease detected at the schizont stage, as previously reported using semiquantitative RT-PCR (20). Moreover, maximum and minimum *g6pd* expression values also showed a two-fold difference.

Our findings indicate that real-time RT-PCR using molecular beacons is a suitable method to assess the in vitro transcriptional regulation of genes expressed both at low levels, such as *g6pd*, and at high levels, such as *Fe-sod*, in *P. falciparum*. The method requires an amount of parasite culture (12 μ L) appropriate for high-throughput analysis. Using robotic devices to extract RNA and produce cDNA, the method proved to be sufficiently sensitive and reproducible to quantify gene expression in the erythrocytic stages of *P. falciparum* infection.

ACKNOWLEDGMENTS

We thank Nuria Trinidad for excellent technical assistance with the parasite cultures. This research was funded by grant nos. PM1999-0049-CO2-01 and BIO2003-07179 (to J.M.B.) from the Spanish Ministry of Science and Technology. L.Y.B. holds a predoctoral fellowship from the Infectious Diseases Program, Fundación Carolina, Spain.

REFERENCES

1. Gardner, M.J., N. Hall, E. Fung, O. White, M. Berriman, R.W. Hyman, J.M. Carlton, A. Pain, et al. 2002. Genome sequence of the human malaria parasite *Plasmodium*

- falciparum*. *Nature* 419:498-511.
2. Florens, L., M.P. Washburn, J.D. Raine, R.M. Anthony, M. Grainger, J.D. Haynes, J.K. Moch, N. Muster, et al. 2002. A proteomic view of the *Plasmodium falciparum* life cycle. *Nature* 419:520-526.
3. Tyagi, S. and F.R. Kramer. 1996. Molecular beacons: probes that fluoresce upon hybridization. *Nat. Biotechnol.* 14:303-308.
4. Giesendorf, B.A., J.A. Vet, S. Tyagi, E.J. Mensink, F.J. Trijbels, and H.J. Blom. 1998. Molecular beacons: a new approach for semiautomated mutation analysis. *Clin. Chem.* 44:482-486.
5. Piatek, A.S., S. Tyagi, A.C. Pol, A. Telenti, L.P. Miller, F.R. Kramer, and D. Alland. 1998. Molecular beacon sequence analysis for detecting drug resistance in *Mycobacterium tuberculosis*. *Nat. Biotechnol.* 16: 359-363.
6. Tyagi, S., D.P. Bratu, and F.R. Kramer. 1998. Multicolor molecular beacons for allele discrimination. *Nat. Biotechnol.* 16: 49-53.
7. Vet, J.A., A.R. Majithia, S.A. Marras, S. Tyagi, S. Dube, B.J. Poesz, and F.R. Kramer. 1999. Multiplex detection of four pathogenic retroviruses using molecular beacons. *Proc. Natl. Acad. Sci. USA* 96: 6394-6399.
8. Durand, R., J. Eslahpazire, S. Jafari, J.F. Delabre, A. Marmorat-Khuong, J.P. Di Piazza, and J. Le Bras. 2000. Use of molecular beacons to detect an antifolate resistance-associated mutation in *Plasmodium falciparum*. *Antimicrobial Agents Chemother.* 44:3461-3464.
9. Liu, J., P. Feldman, and T.D. Chung. 2002. Real-time monitoring in vitro transcription using molecular beacons. *Anal. Biochem.* 300:40-45.
10. Marras, S.A., F.R. Kramer, and S. Tyagi. 1999. Multiplex detection of single nucleotide variations using molecular beacons. *Genet. Anal.* 14:151-156.
11. Szemes, M. and C.D. Schoen. 2003. Design of molecular beacons for AmpliDet RNA assay—characterization of binding stability and probe specificity. *Anal. Biochem.* 315: 189-201.
12. Bustin, S. 2000. Absolute quantification of mRNA using real-time reverse transcription polymerase chain reaction assays. *J. Mol. Endocrinol.* 25:169-193.
13. Tsourkas, A., M.A. Behlke, S.D. Rose, and G. Bao. 2003. Hybridization kinetics and thermodynamics of molecular beacons. *Nucleic Acids Res.* 31:1319-1330.
14. Witney, A.A., D.L. Doolan, R.M. Anthony, W.R. Weiss, S.L. Hoffman, and D.J. Carucci. 2001. Determining liver stage parasite burden by real-time quantitative PCR as a method for evaluating pre-erythrocytic malaria vaccine efficacy. *Mol. Biochem. Parasitol.* 118:233-245.
15. Hermsen, C.C., D.S. Telgt, E.H. Linders, L.A. van de Locht, W.M. Eling, E.J. Mensink, and R.W. Sauerwein. 2001. Detection of *Plasmodium falciparum* malaria in vivo by real-time quantitative PCR. *Mol. Biochem. Parasitol.* 118:247-251.
16. Trager, W. and J.B. Jensen. 1976. Human malaria parasites in continuous culture. *Science* 193:673-675.
17. Lambros, C. and J.P. Vanderberg. 1979. Synchronization of *Plasmodium falciparum* erythrocytic stages in culture. *J. Parasitol.* 65:418-420.
18. Zuker, M. 2003. Mfold web server for nucleic acid folding and hybridization prediction. *Nucleic Acids Res.* 31:3406-3415.
19. Bonnet, G., S. Tyagi, A. Libchaber, and F.R. Kramer. 1999. Thermodynamic basis of the enhanced specificity of structured DNA probes. *Proc. Natl. Acad. Sci. USA* 96: 6171-6176.
20. Calvo, E., C. Rubiano, A. Vargas, and M. Wasserman. 2002. Expression of housekeeping genes during the asexual cycle of *Plasmodium falciparum*. *Parasitol. Res.* 88: 267-271.

Received 22 August 2003; accepted 31 December 2003.

Address correspondence to José M. Bautista, Departamento de Bioquímica y Biología Molecular IV, Universidad Complutense de Madrid, Facultad de Veterinaria, Ciudad Universitaria, 28040 Madrid, Spain. e-mail: jmbau@vet.ucm.es